Supporting Information

Copper(I)iodide coordination polymers with triazole substituted pyridine ligands: Photophysical and electrical conductivity properties

Shivendu Mishra[a], Dilip Pandey[a], Kulbhushan Mishra[b], Lydie Viau[c] and Abhinav Raghuvanshi*[a]

[a]*Department of Chemistry, Indian Institute of Technology Indore, 453552, Madhya Pradesh, India.* Email: r.abhinav@iiti.ac.in

[b]*Department of Physics, Indian Institute of Technology Indore, 453552, Madhya Pradesh, India.*

[c]*Université de Franche-Comté, CNRS, Institut UTINAM, F-25000 Besançon, France*

Table of contents

General Information

Materials

All reactions were performed in an oven-dried two-neck round bottom (r.b.) flask Schlenk tube, kept at 80 °C a day prior to use and the reactions were performed using Schlenk line technique under N_2 atmosphere. Materials required for the synthesis of ligands such as 2-bromopyridine (>99%), 3-bromopyridine (>99%), 4-bromopyridine hydrochloride (>98%) were bought from Spectrochem (India) and used without further purification. Cesium carbonate (>99%), CuI (>99%) were bought from Loba Chemie Pvt. Ltd., CuO (>98%) and potassium carbonate (>99%) were purchased from Avra Synthesis Pvt. Ltd. Solvents like dimethyl formamide (DMF), dimethyl sulfoxide (L.R. grade) were bought from Advent Chembio Pvt. Ltd., acetonitrile HPLC grade from Finar Chemicals Pvt. Ltd. and deuterated solvents DMSO-d_6, $CDCl_3$ with 0.03 % TMS as an internal standard were from Eurisotop.

Characterization methods

A Bruker Avance (III) spectrometer operating at 400 MHz was used for the characterization of synthesized ligands. The ligand purity was confirmed by high-performance liquid chromatography (HPLC) using Waters HPLC having 2298 PDA detector along with flex inject injector. Single crystal X-Ray data for structural analysis were obtained on dual source Super Nova CCD, Agilent Technologies (Oxford Diffraction) System using Mo-Kα= 0.71073 at 293 K. The structure solution was obtained by using OLEX software and the SHELXT structure solution program using Intrinsic Phasing and refined with the SHELXL refinement package using Least Squares.[1,2] Fluorescence quantum yield of the solid samples were measured using an integral sphere set up coupled with a Jobin Yvon Horiba Model Fluorolog-3-21 (Xenon lamp 450 W). The crystallinity and phase purity measurements of all three coordination polymers were performed on a Rigaku Smart X-ray diffractometer with monochromatic Cu Kα (0.1540 nm) radiation in 2θ range of 5-50 degrees. Bruker Alpha II spectrophotometer was used for FT-IR and Keithley model 6517B electrometer for conductivity experiments. The thermogravimetric analysis was performed on Mettler Toledo TGA/DSC 1 star e- system in the temperature range of 30-800 °C.

Synthetic procedure for L^1, L^2, L^3, CP1, CP2 and CP3

Synthesis of L^1. 2-(1H-1,2,4-triazol-1-yl)pyridine (L^1) was synthesized by following a reported procedure.[3] To an oven-dried two-neck round bottom flask (r.b.), were added 1H-1,2,4-triazole (4.8 mmol, 331.5 mg), Cs_2CO_3 (6.138 mmol, 2g), CuI (0.76 mmol, 145 mg) and 2-bromopyridine (4 mmol, 395 µL). The resulting mixture was stirred and heated at 140 °C for 40 h. The reaction mixture was cooled down to room temperature, diluted with ethyl acetate and passed through a celite pad. The product was washed with a brine solution and water. The final product was passed through column charged with silica by using hexane : ethyl acetate (2:3 by volume) as eluent, to get the desired product in 87 % yield. The sample purity was analysed using acetonitrile:deionized water in different (V/V) ratios in isocratic mode (**Fig. S1-S2**). ^{1}H NMR (400 MHz, $CDCl_3$) δ (ppm) 9.18 (s, 1H), 8.46 (d, J = 4.3Hz, 1H,), 8.10 (s, 1 H), 7.90 (d, J = 6.4 Hz, 2 H), 7.31 (s, 1H).

Synthesis of L^2. 3-(1H-1,2,4-triazol-1-yl)pyridine (L^2) was synthesized with a slight modification from the reported literature procedure.[4] To a dried two-neck r.b. charged with N_2, 1H-1,2,4-triazole (3.79 mmoL, 262.59 mg), K_2CO_3 (3.79 mmol, 525 mg), CuO (0.379 mmol, 30.2 mg) and 3-bromopyridine (3.164mmol, 307.7 µL) were added and heated at 150 °C for 72 h. The reaction mixture was diluted with dichloromethane (DCM) and washed with brine solution and water. After drying, the solvent was evaporated under vacuum. The obtained product was recrystallized with DCM-hexane to get the pure product in 74% yield asl off-white solid. The sample purity was analysed using HPLC using acetonitrile solvent with deionized water in different (V/V) ratios in isocratic mode (**Fig. S1-S2**). ^{1}H NMR (400 MHz, $CDCl_3$) δ (ppm) 8.98 (s, 1 H), 8.64 (d, J = 4.5, 1 H), 8.62 (s, 1 H), 8.13 (s, 1 H), 8.02 (d, J = 8.0, 1 H), 7.53 – 7.41 (m, 1 H).[5]

Synthesis of L^3. 4-(1H-1,2,4-triazol-1-yl)pyridine (L^3) was synthesized with a slight modification from the reported literature procedure.[3] First, in a dried two neck r.b. flask, was added 4-bromopyridine·HCl (10 mmol, 1945 mg) and Cs_2CO_3 (19.82 mmol, 6.46 g). The mixture was heated at 140 °C for 12 h to get 4-bromopyridine. After that, 1H-1,2,4-triazole (14 mmoL, 967 mg) and CuI (0.9 mmol, 180 mg) were added and the resulting mixture was stirred for another 48 hours. The reaction was cooled down to room temperature, diluted with DCM and filtered on celite pad. The product was washed with brine and the solvent was removed under vacuum. The sample purity was analysed using HPLC using acetonitrile solvent with deionized water in different (V/V)

ratios in isocratic mode (**Fig. S1-S2**). ^{1}H NMR (400 MHz, $CDCl_3$) δ (ppm) 9.60 (s, 1 H), 8.84 – 8.78 (m, 2 H), 8.41 (s, 1 H), 7.99 (d, J = 5.4, 2 H).[5]

Synthesis of 1D $[Cu_2I_2(L^1)_2]_n$ CP1. To a solution of CuI (65mg, 0.34mmol) in CH_3CN (3mL) was added **L^1** (50 mg, 0.34mmol) in CH_3CN (2mL). A white precipitate was observed within 1-2 minutes. The mixture was further stirred for 45 minutes to complete the reaction. The precipitate was filtered and washed with dichloromethane and CH_3CN (1mL) 2-3 times and then dried over the vacuum. Overall yield = 80%. A small amount of **CP1**, about 20mg, was dissolved in hot CH_3CN and left to grow crystals. After a week, colourless needle-shaped crystals suitable for SCXRD were obtained.

Synthesis of 1D $[Cu_2I_2(L^2)_2]_n$ CP2. CP2 was prepared in a manner like **CP1** using **L^2**, giving an overall yield of 49%. A small amount of **CP2** (20mg) was dissolved in hot CH_3CN and left to grow crystals. After a few days, yellow crystals appeared compatible with single-crystal X-ray diffraction.

Synthesis of 1D $[CuI(L^3)]_n$ CP3. CP3 was prepared following the same procedure as **CP1** except **L^3**, giving a yellow powder with an overall yield of up to 60%. Crystals of **CP3** were obtained by layering an aqueous solution of KI, CuI and an ethanol solution of ligand [4-(1H-1,2,4triazol-1-yl)pyridine] with CH_3CN buffer in the middle. Yellow rod-like crystals suitable for SCXRD were obtained after 7-10 days.

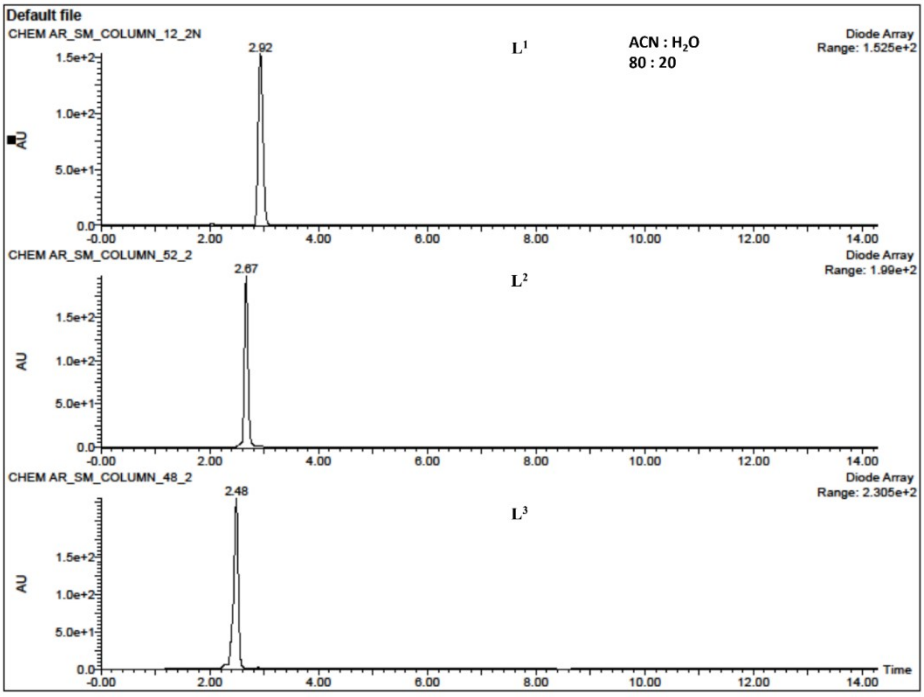

Fig. S1. Sample purity, characterized by HPLC in isocratic mode using ACN:H_2O (80:20) V/V ratio.

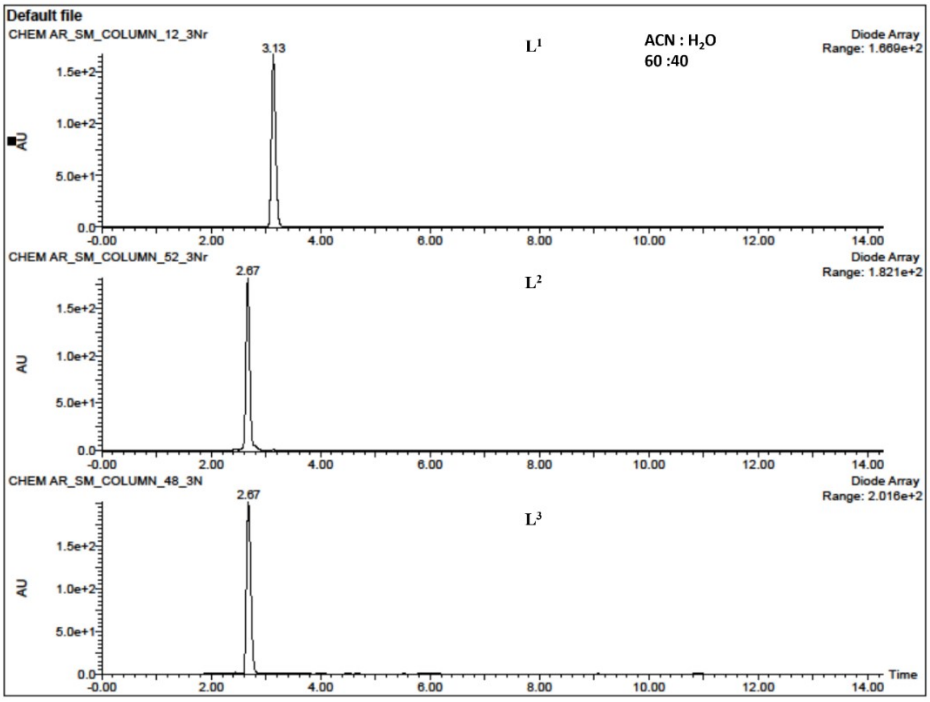

Fig. S2. Sample purity, characterized by HPLC in isocratic mode using ACN:H_2O (60:20) V/V ratio.

Table S1. Crystal and refinement data table of **CP1**, **CP2** and **CP3**.

	CP1 (2Tz)	**CP2** (3Tz)	**CP3** (4Tz)
CCDC No.	2262590	2262602	2262603
Empirical formula	$C_7H_6CuIN_4$	$C_7H_6CuIN_4$	$C_7H_6CuIN_4$
Formula weight	336.60	336.60	336.60
Temperature (K)	293(2)	300(2)	298(2)
Crystal system	Monoclinic	Triclinic	Monoclinic
Space group	$P2_1/c$	$P\bar{1}$	$P2_1/c$
Z	4	2	4
a (Å)	4.1874(2)	7.8402(4)	4.31310(10)
b (Å)	20.8052(11)	8.1337(5)	16.4341(6)
c (Å)	11.0045(8)	9.0972(4)	12.8515(4)
α (°)	90	107.503(4)	90
β (°)	94.281(5)	101.344(4)	97.980(3)
γ (°)	90	113.872(6)	90
V (Å^3)	956.03(10)	471.01(5)	902.12(5)
D_{calc} (g/cm^3)	2.339	2.373	2.478
$2\theta_{max}$ (°)	58.41	56.996	58.342
R1, wR2 [I>2σ(I)]	0.0563, 0.1538	0.0393, 0.0937	0.0292, 0.0656
R1, wR2 [all data]	0.0714, 0.1627	0.0540, 0.1010	0.0351, 0.0698
Goodness-of-fit on F^2	1.099	1.076	1.056
No. of reflection used[>2σ(I)]	3701 [R_{int} = 0.0502]	2300 [R_{int}= 0.0661]	2236 [R_{int} = 0.0464]

Table S2. Bond-lengths (Å) of **CP1**.

Cu1- Cu1^1	2.900 (2)	N2- C7	1.345 (12)
Cu1- Cu1^2	2.750 (3)	N3- C6	1.306 (13)
Cu1- N4	2.038 (7)	N4- C6	1.359 (11)
Cu1- I1	2.6466 (15)	N4- C7	1.296 (12)
Cu1- I1^1	2.6538 (13)	C1- C2	1.3900
Cu1^2- I1	2.6639 (14)	C2- C3	1.3900
N1- C1	1.3900	C3- C4	1.3900
N1- C5	1.3900	C4- C5	1.3900
N2- N3	1.352 (11)	I1- Cu1^1	2.6538 (13)
N2- C1	1.355 (8)	I1- Cu1^2	2.6639 (14)

Where, symmetry operation (1) -*x*,1-*y*, -*z*, (2) -*x*,1-*y*,-*z*

Table S3. Bond angles (°) for **CP1**.

Cu1-I1-Cu1^1	62.51 (5)	N3-N2-C1	119.6(7)
Cu1-I1-Cu1^2	66.20 (5)	C7-N2-N3	110.3 (8)
Cu1^1-I1-Cu1^2	103.89 (5)	C7-N2-C1	130.1 (8)

I1-Cu1-I1[1]	117.49 (5)	C6-N3-N2	101.9 (8)
I1-Cu1-I1[2]	113.80 (5)	C6-N4-Cu1	126.9 (6)
I1[1]-Cu1-I1[2]	103.89 (5)	C7-N4-Cu1	129.3 (6)
I1-Cu1-Cu1[1]	58.88 (5)	C7-N4-C6	103.8 (8)
I1-Cu1-Cu1[2]	57.19 (4)	N2-C1-N1	115.5 (5)
I1[2]-Cu1-Cu1[1]	128.32 (7)	N2-C1-C2	124.5 (5)
I1[2]-Cu1-Cu1[2]	56.61 (4)	N1-C1-C2	120.0
I1[1]-Cu1-Cu1[2]	129.93 (7)	C1-N1-C5	120.0
I1[1]-Cu1-Cu1[1]	58.62 (5)	C4-C5-N1	120.0
Cu1[1]-Cu1-Cu1[2]	95.62 (7)	C3-C4-C5	120.0
N4-Cu1-I1	104.6 (2)	C4-C3-C2	120.0
N4-Cu1-I1[2]	108.0 (2)	C3-C2-C1	120.0
N4-Cu1-I1[1]	108.8 (2)	N3-C6-N4	114.7 (9)
N4-Cu1-Cu1[2]	120.9 (2)	N4-C7-N2	109.3 (8)
N4-Cu1-Cu1[1]	123.6 (2)		

Symmetry operation code (1) -*x*,1-*y*,-*z* (2) 1-*x*,1-*y*,-*z*

Table S4. Bond-lengths (Å) of **CP2**.

I1- Cu1	2.6848 (7)	N2- C7	1.329 (6)
I1- Cu1[1]	2.7381 (8)	N3- C6	1.321 (7)
Cu1- I1	2.7381 (8)	N4- Cu1[3]	2.023 (4)
Cu1- Cu1[1]	2.8478 (14)	N4- C6	1.337 (7)
Cu1- N1	2.021 (4)	C1- C2	1.375 (6)
Cu1- N4[2]	2.023 (4)	C2- C3	1.390 (8)
N1- C1	1.343 (6)	C3- C4	1.383 (7)
N1- C5	1.350 (6)	C4- C5	1.378 (7)
N2- N3	1.372 (6)	N4-C7	1.307 (6)
N2- C1	1.424 (6)		

Where, symmetry operation (1) 1-*x*, 1-*y*, -*z* (2) -1+*x*, -1+*y*, -1+*z* (3) 1+*x*, 1+*y*, 1+*z*

Table S5. Bond angles (°) for **CP2**.

Cu1-I1-Cu1[1]	63.35 (3)	C7-N2-N3	108.9 (4)
I1- Cu1-I1[1]	116.66 (3)	C7-N2-C4	131.0 (4)
I1[1]- Cu1-Cu1[1]	57.42 (2)	C6-N3-N2	101.7 (4)
I1- Cu1-Cu1[1]	59.24 (2)	C6-N4-Cu1[3]	123.7 (3)
N1- Cu1-I1[1]	99.94 (12)	C7-N4- Cu1[3]	130.8 (4)
N1- Cu1-I1	107.02 (12)	C7-N4-C6	103.0 (4)
N1- Cu1-Cu1[1]	116.23 (12)	N1-C1-C2	123.2 (4)
N1- Cu1-N4[2]	130.07 (17)	C1-C2-C3	119.6 (5)
N4[2]- Cu1-I1	104.33 (12)	C4-C3-C2	117.1 (5)
N4[2]- Cu1-I1[1]	99.46 (12)	C3-C4-N2	120.1 (5)
N4[2]- Cu1-Cu1[1]	113.04 (13)	C5-C4-N2	119.3 (4)
C1-N1-Cu1	121.0 (3)	C5-C4-C3	120.6 (4)
C1-N1-C5	117.4 (4)	N1-C5-C4	122.0 (4)
C5-N1-Cu1	121.1 (3)	N3-C6-N4	115.3 (5)
N3-N2-C4	120.1 (4)	N4-C7-N2	111.2 (4)

Symmetry operation code (1) 1-*x*, 1-*y*, -*z* (2) -1+*x*, -1+*y*, -1+*z* (3) 1+*x*, 1+*y*, 1+*z*

Table S6. Bond-lengths (Å) of **CP3**.

I1- Cu1	2.6478 (5)	N2- C3	1.420 (4)
I1- Cu1[1]	2.6796 (5)	N2- C6	1.337 (5)
Cu1- I1[2]	2.6796 (5)	N3- C7	1.313 (5)
Cu1- N1[3]	2.042 (3)	N4- C6	1.324 (4)
Cu1- N4	2.043 (3)	N4-C7	1.366 (5)
N1- Cu1[4]	2.042 (3)	C1- C2	1.373 (5)
N1- C1	1.336 (5)	C2- C3	1.389 (4)
N1- C5	1.331 (4)	C3- C4	1.366 (5)
N2- N3	1.368 (4)	C4- C5	1.380 (5)

Where, symmetry operation (1) -1+*x*, +*y*, +*z* (2) 1+*x*, +*y*, +*z* (3) 1-*x*, 1/2+*y*, 1/2-*z* (4) 1-*x*, -1/2+*y*, 1/2-*z*

Table S7. Bond angles (°) for **CP3**.

Cu1-I1-Cu1[1]	108.115 (17)	C7-N3-N2	102.6 (3)
I1- Cu1-I1[2]	108.115 (17)	C6-N4-Cu1	133.2 (3)
N1[3]- Cu1-I1[2]	102.69 (8)	C6-N4-C7	102.4 (3)
N1[3]- Cu1-I1	111.44 (8)	C7-N4- Cu1	124.3 (2)
N1[3]- Cu1-N4	113.46 (12)	N1-C1-C2	124.2 (3)
N4- Cu1-I1	106.83 (8)	C1-C2-C3	117.9 (3)
N4- Cu1-I1[2]	114.27 (8)	C2-C3-N2	120.8 (3)
C1-N1-Cu1[4]	124.3 (2)	C4-C3-N2	119.8 (3)
C5-N1-Cu1[4]	119.1 (3)	C4-C3-C2	119.4 (3)
C5-N1-C1	116.2 (3)	C3-C4-C5	118.0 (3)
N3-N2-C3	119.8 (3)	N1-C5-C4	124.4 (4)
C6-N2-N3	109.3 (3)	N4-C6-N2	110.8 (3)
C6-N2-C3	130.8 (3)	N3-C7-N4	114.9 (3)

Symmetry operation code (1) -1+*x*, +*y*, +*z* (2) 1+*x*, +*y*, +*z* (3) 1-*x*, 1/2+*y*, 1/2-*z* (4) 1-*x*, -1/2+*y*, 1/2-z

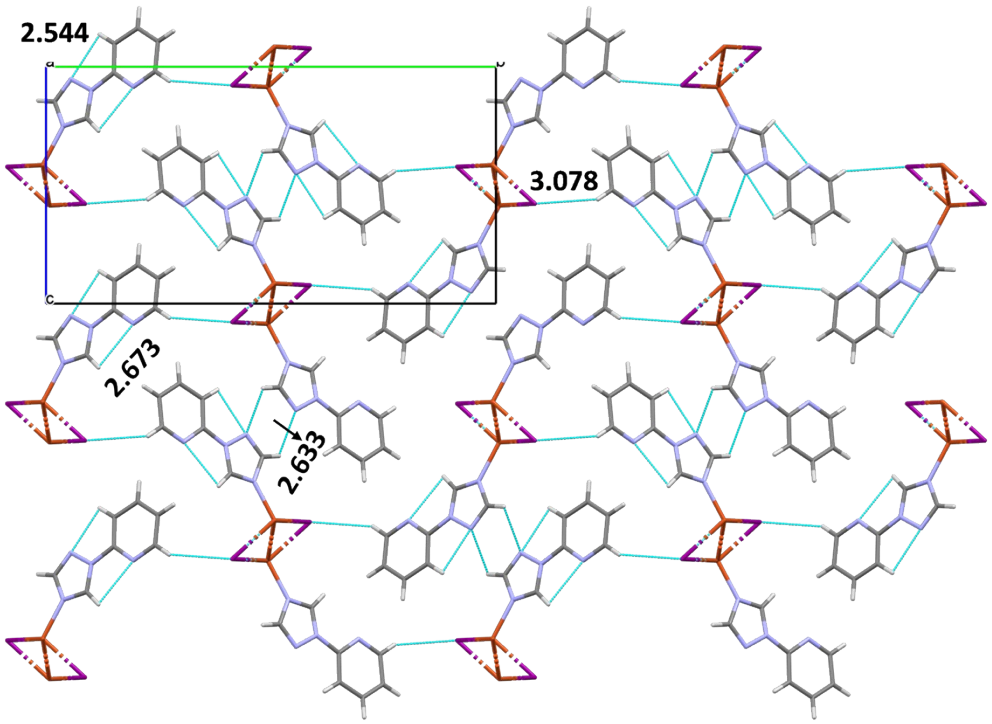

Fig. S3. Packing of **CP1** along *a* axis and dashed lines showing C-H---I and C-H---N interactions present between the layers.

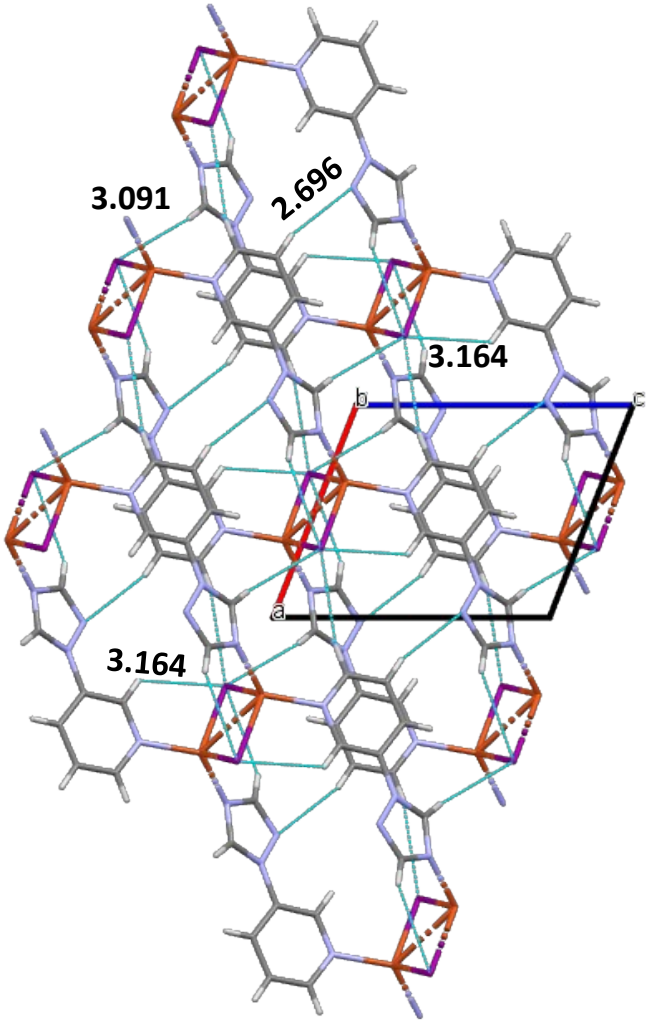

Fig. S4. Packing of **CP2** showing C-H---N, C-H---I interactions along *b* axis.

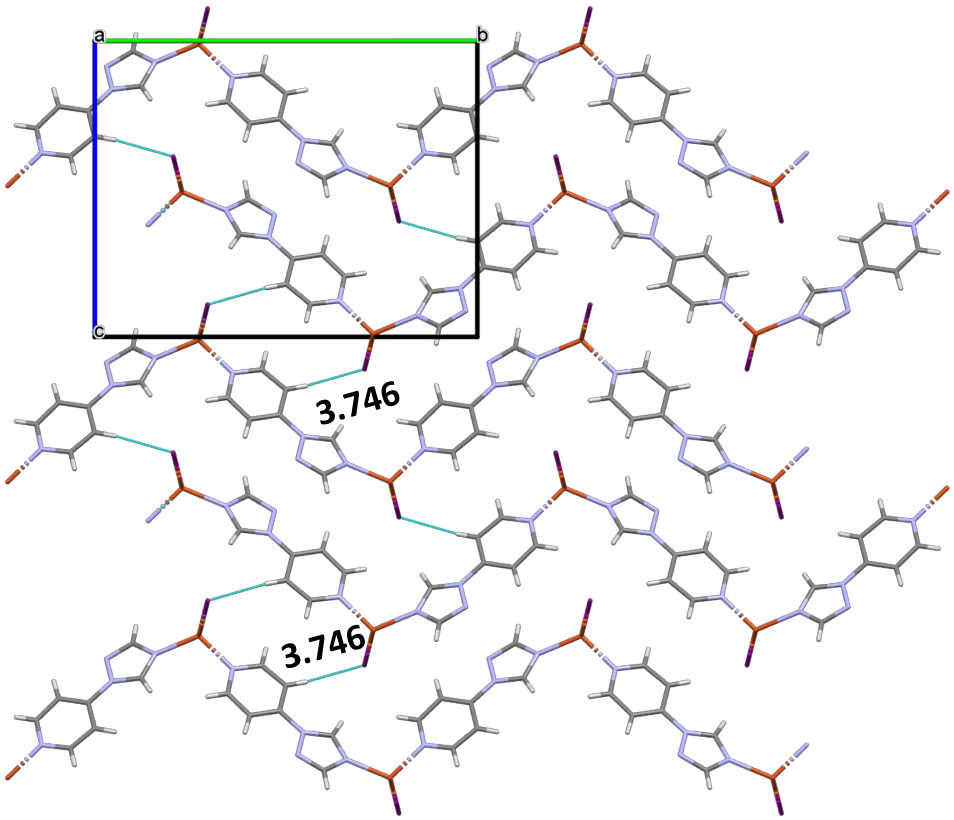

Fig. S5. Packing of **CP3** showing C-H---I interactions along *a* axis.

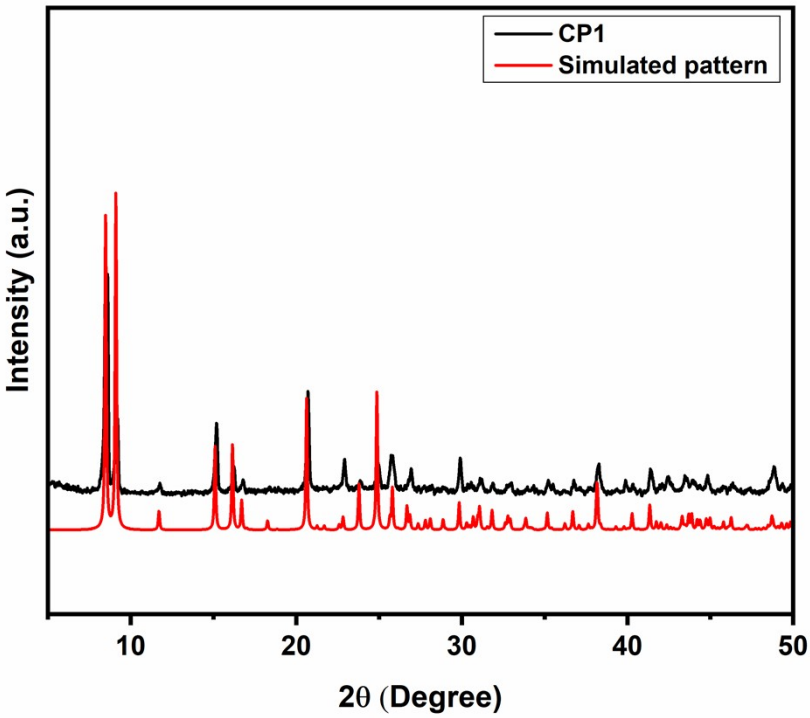

Fig. S6. Comparison of experimental and simulated PXRD patterns of **CP1**.

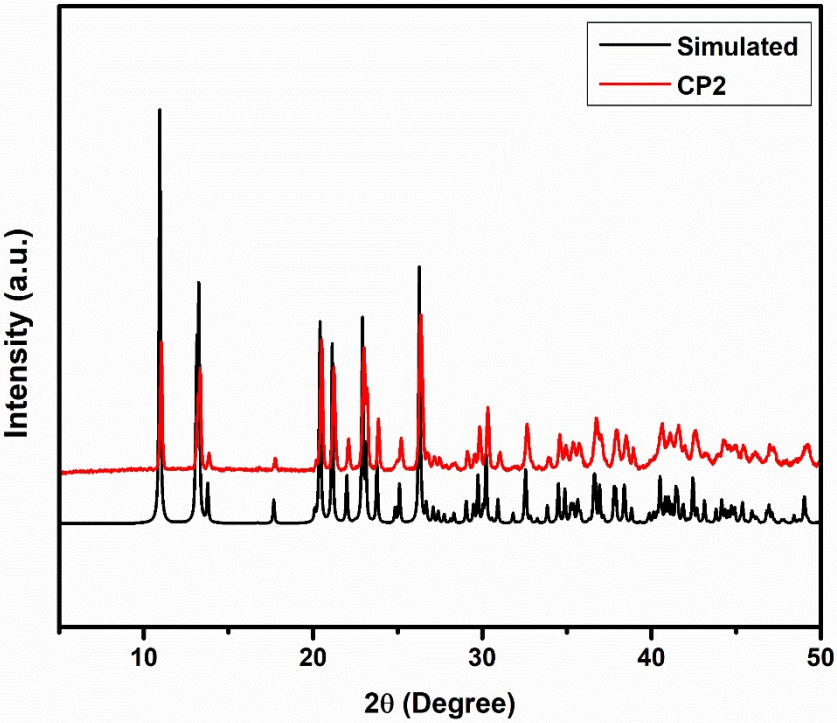

Fig. S7. Comparison of experimental and simulated PXRD patterns of **CP2**.

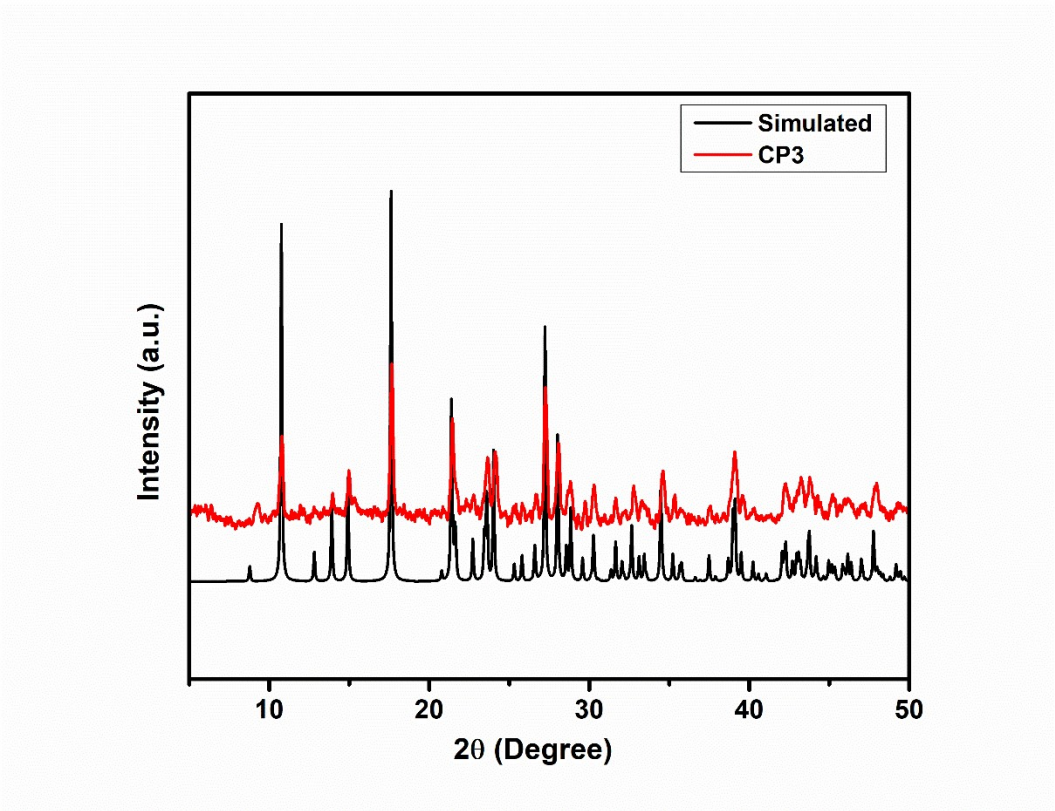

Fig. S8. Comparison of experimental and simulated PXRD patterns of **CP3**.

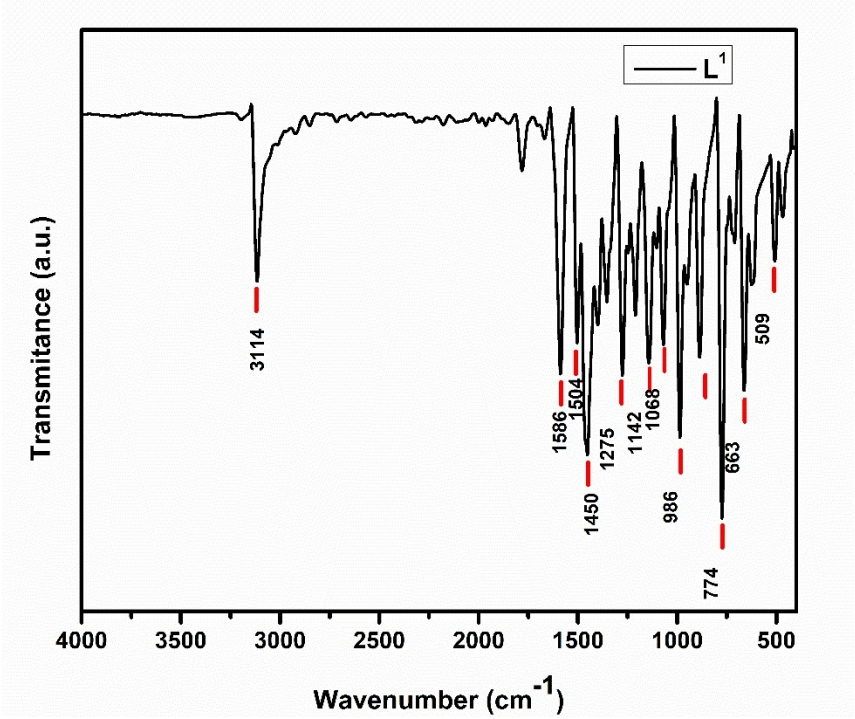

Fig. S9. IR spectrum of $\mathbf{L^1}$.

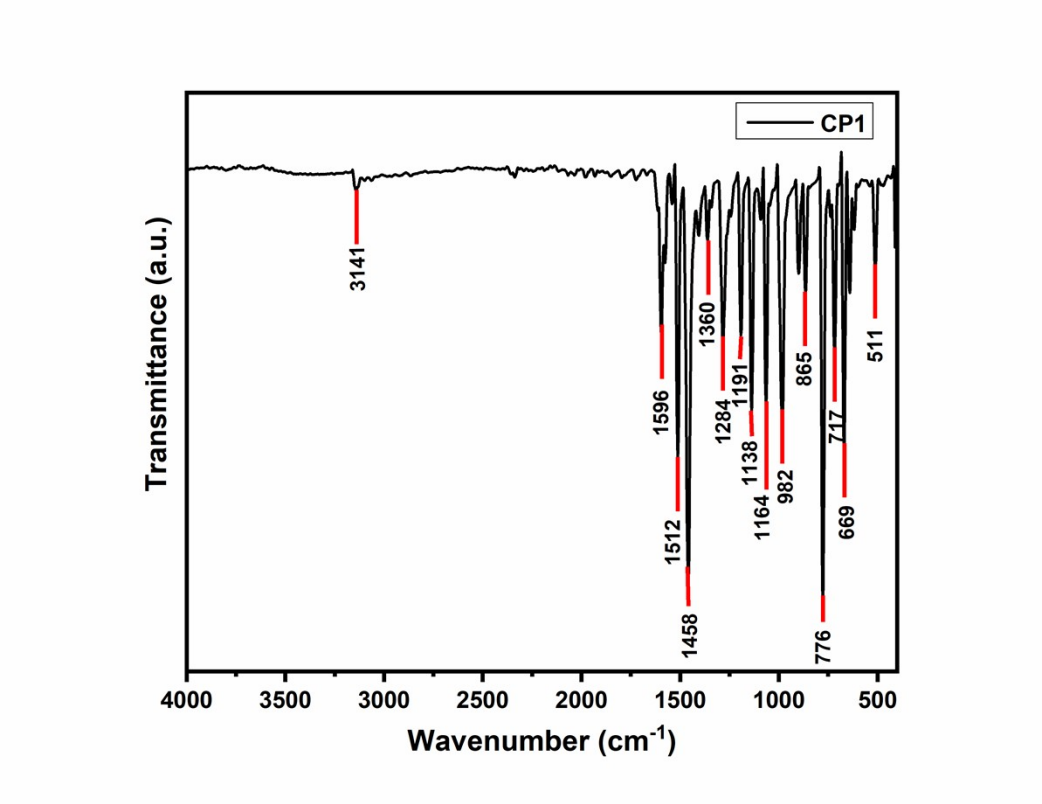

Fig. S10. IR spectrum of **CP1**.

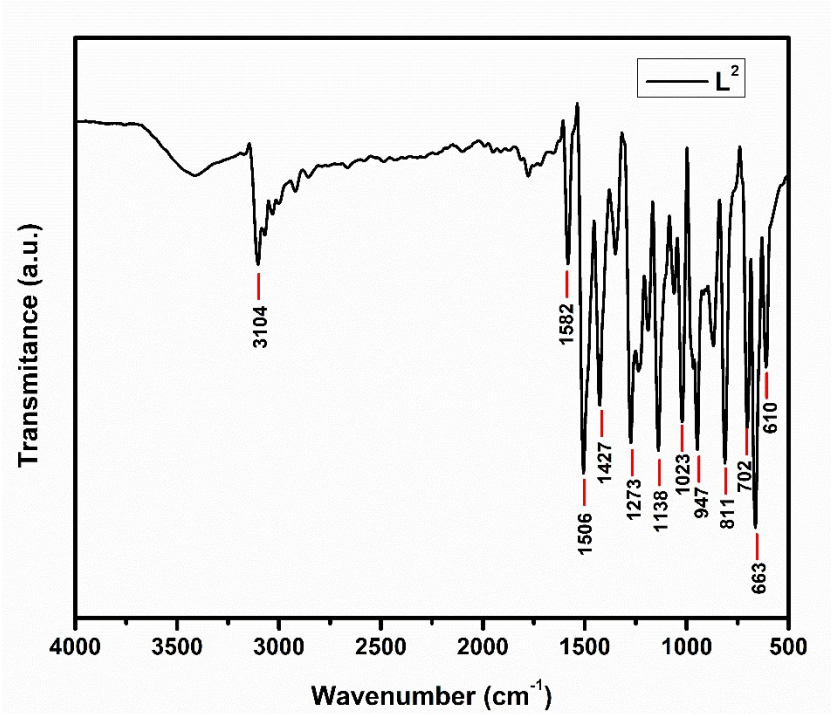

Fig. S11. IR spectrum of $\mathbf{L^2}$.

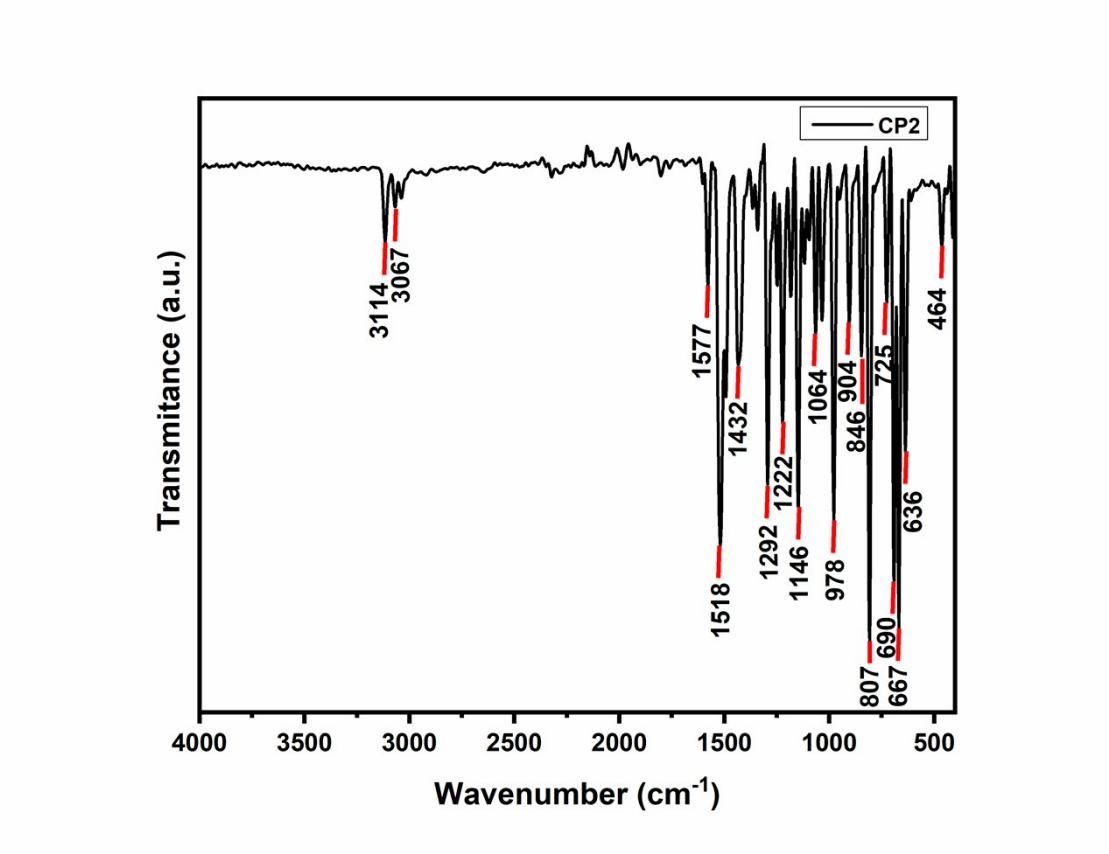

Fig. S12. IR spectrum of **CP2**.

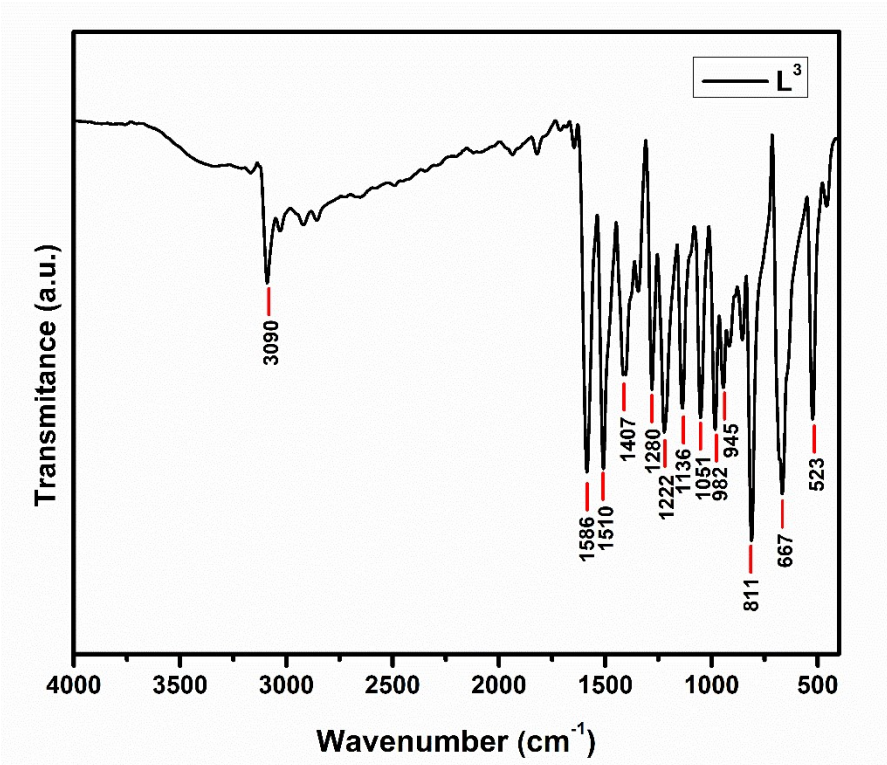

Fig. S13. IR spectrum of $\mathbf{L^3}$.

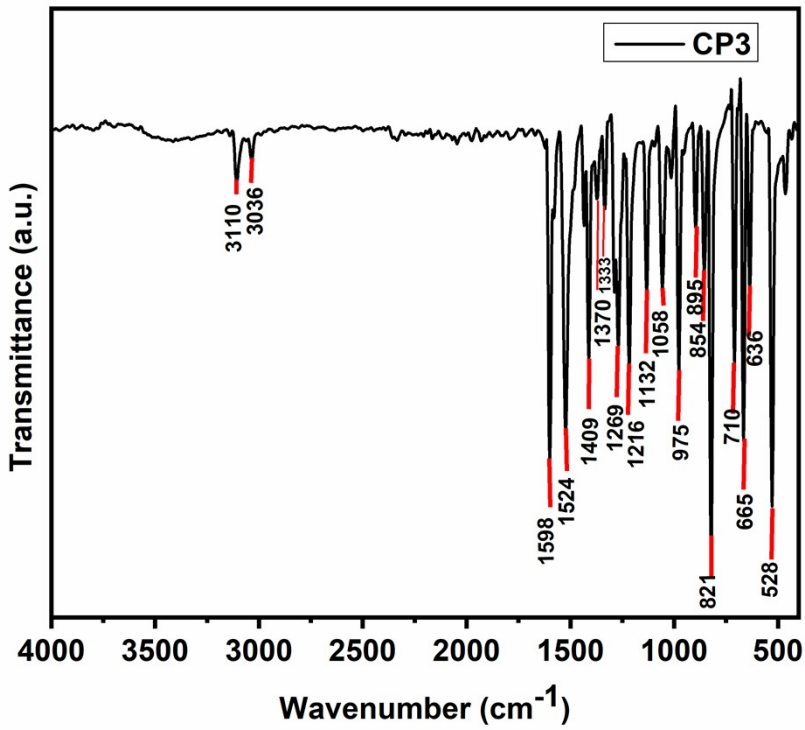

Fig. S14. IR spectrum of **CP3**.

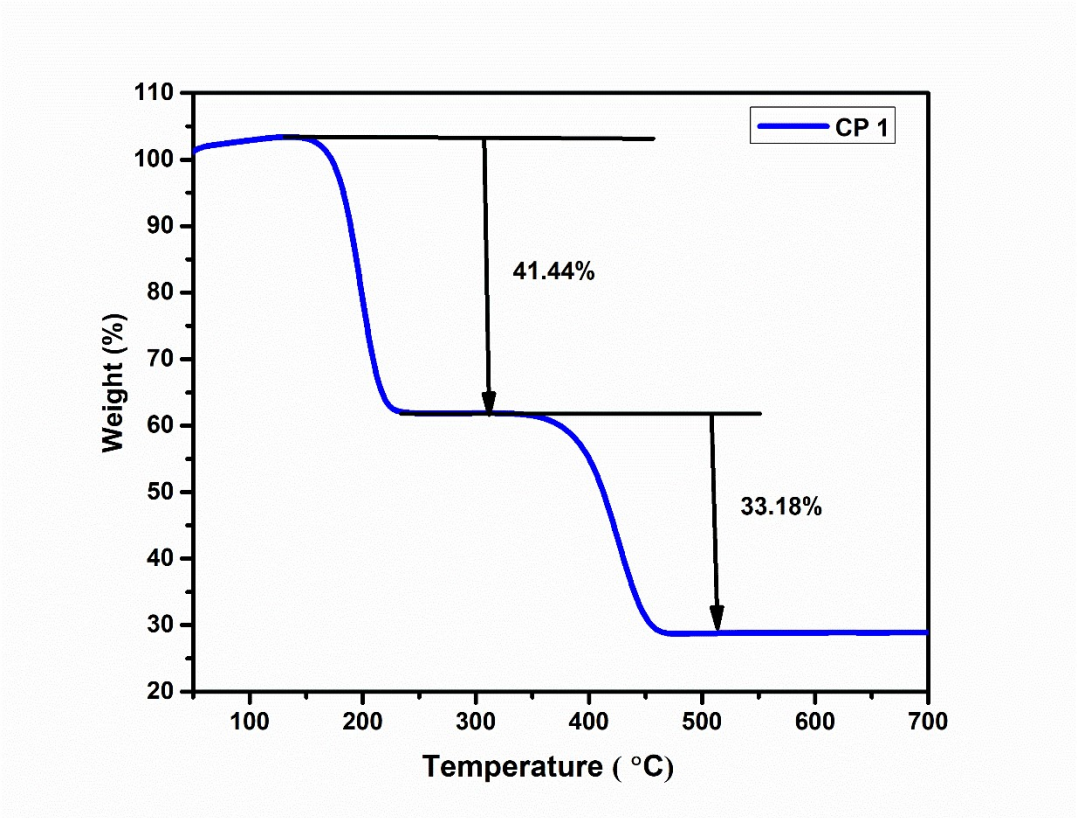

Fig. S15. TGA graph for **CP1**.

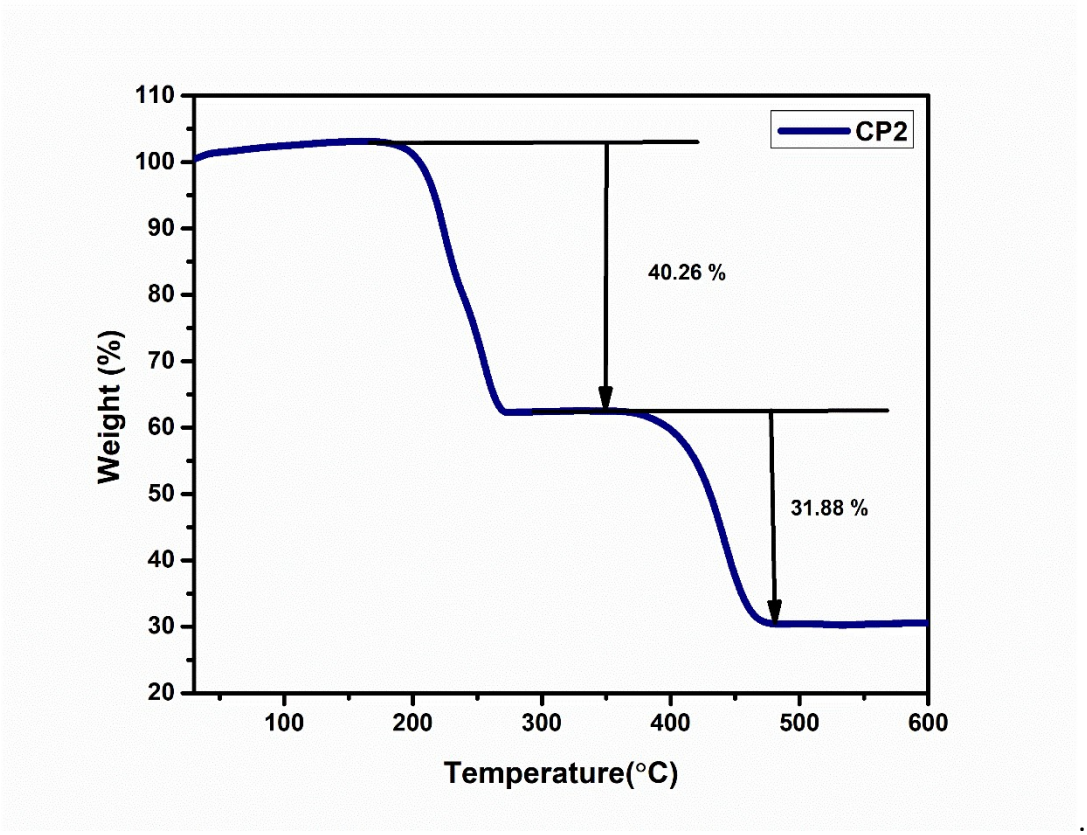

Fig. S16. TGA graph for **CP2**.

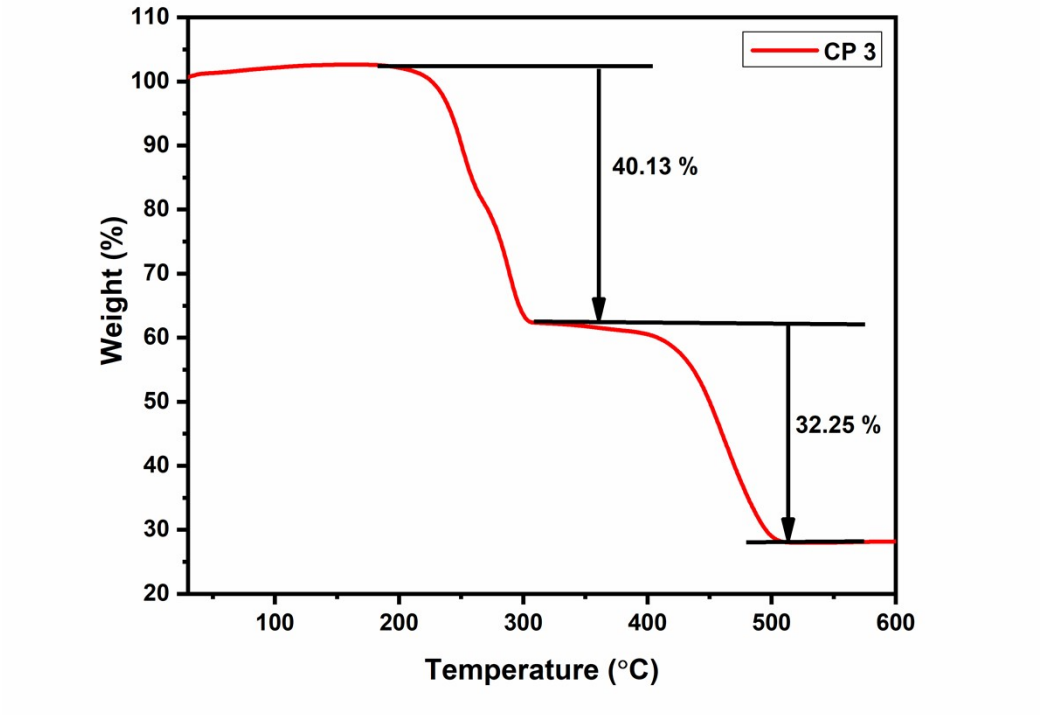

Fig. S17. TGA graph for **CP3**.

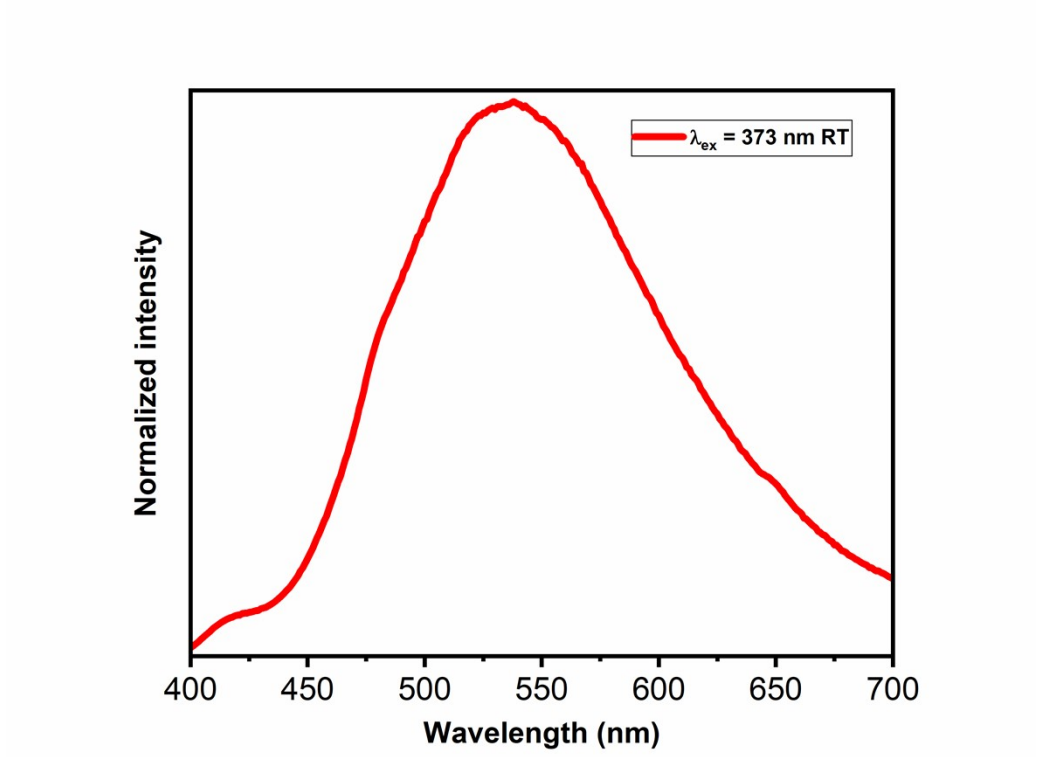

Fig. S18. Emission spectrum of **CP1** at R.T.

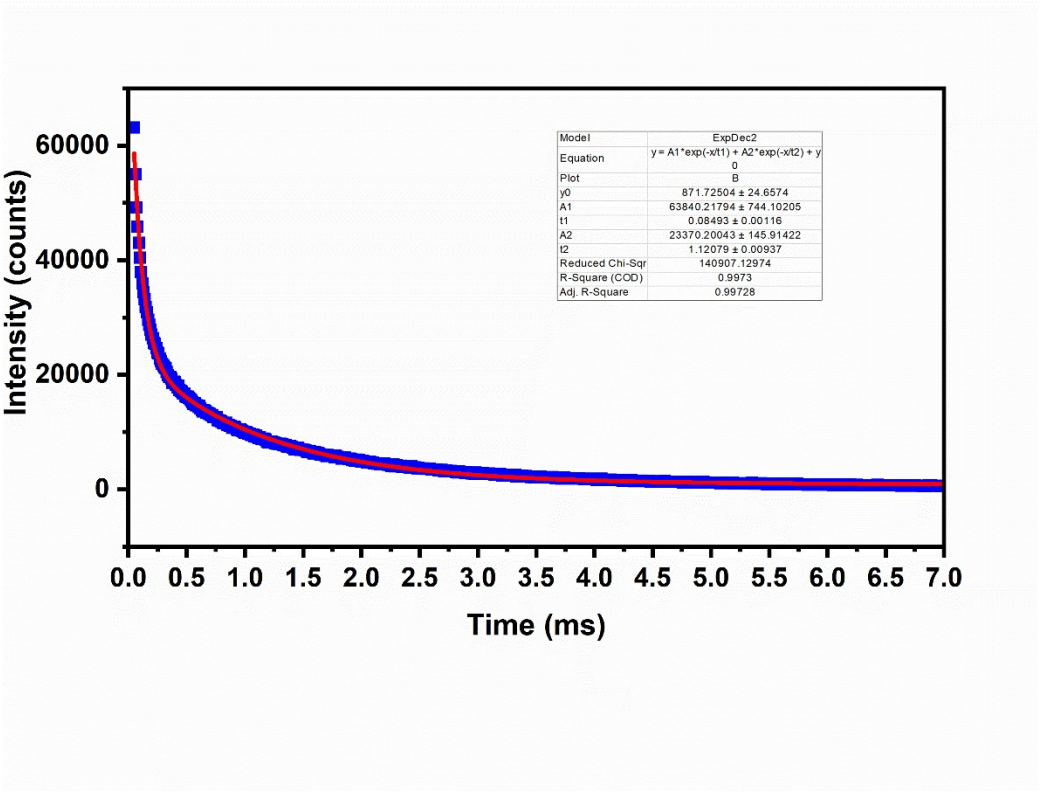

Fig. S19. Lifetime of **CP1** at R.T.

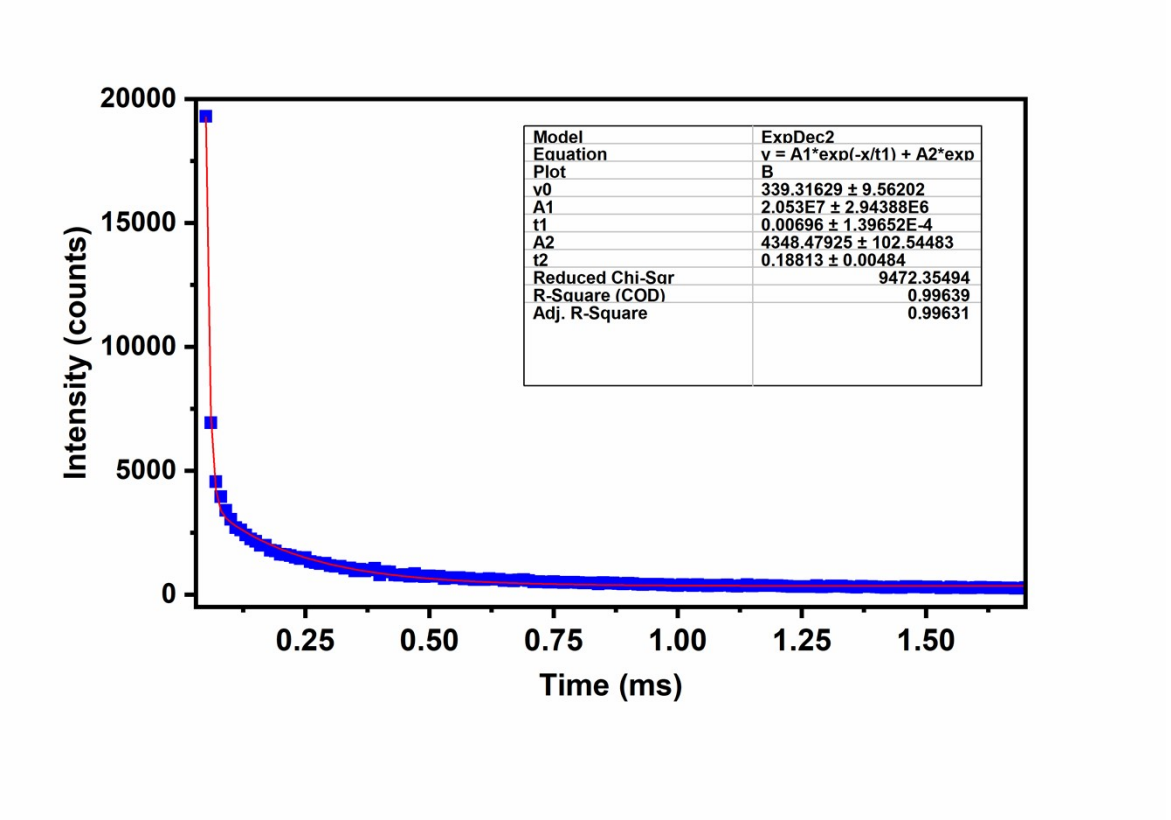

Fig. S20. Lifetime of **CP2** at R.T.

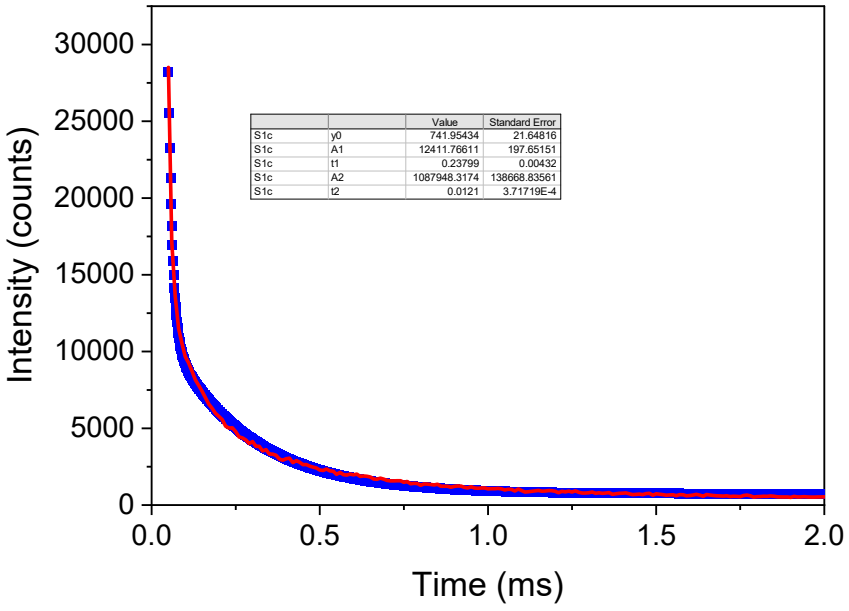

Fig. S21. Lifetime of **CP3** at R.T.

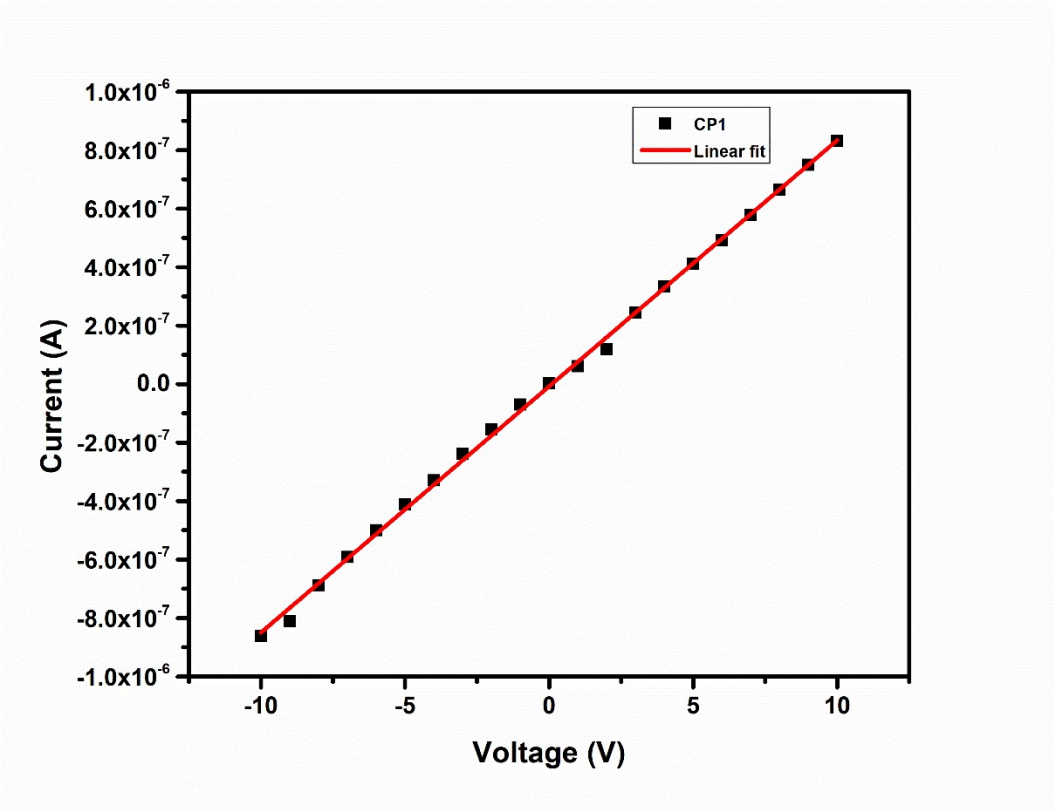

Fig. S22. I *vs* V plot for **CP1**.

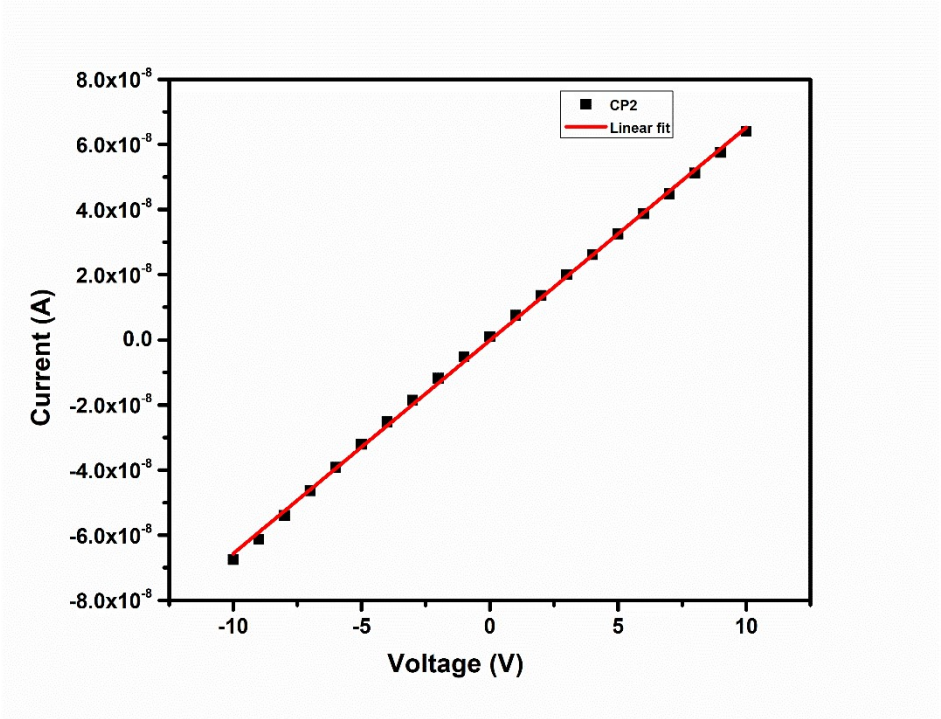

Fig. S23. I *vs* V plot for **CP2**.

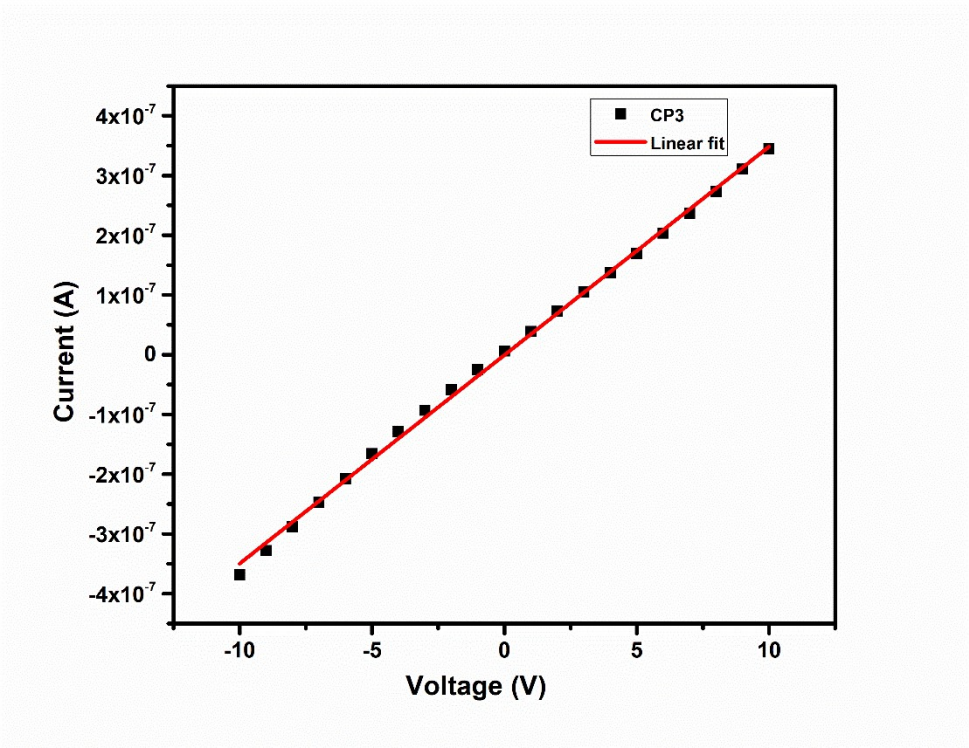

Fig. S24. I *vs* V plot for **CP3**.

Table S8. Comparison of conductivities values for different polymers with Cu_2I_2 core.

Coordination polymers with Cu_2I_2 chain	Conductivities at R.T. (S/cm)	References
$[Cu_2I_2(Apyz)]_n$	8.6×10^{-7}	6
$[CuI(C_5H_5N_3O_2)]_n$	1.1×10^{-8}	7
$[CuI(EtIN)]_n$, $[CuI(MeIN)]_n$	2×10^{-6}, 4×10^{-7}	8
$[Cu(aClpym)I]_n$	1.1×10^{-7}	9
$[Cu_2I_2(Fpyz)]_n$	2.0×10^{-5}	10
$[CuI(HIN)]_n$, $[CuI(Cl\text{-}HIN)]_n$	3.0×10^{-3}, 3.0×10^{-5}	11
$[Cu_2I_2(Fpyz)]_n$	3.1×10^{-5}	12
$[Cu(Cl\text{-}HIN)I]_n$	3.0×10^{-5}	13
CP1	8.85×10^{-7}	**This work**

References

1 G. M. Sheldrick, *Acta Crystallogr. A: Found. Adv.*, 2015, **71**, 3–8.

2 O. V. Dolomanov, L. J. Bourhis, R. J. Gildea, J. a. K. Howard and H. Puschmann, *J. Appl. Cryst.*, 2009, **42**, 339–341.

3 N. Kommu, V. D. Ghule, A. S. Kumar and A. K. Sahoo, *Asian J. Chem.*, 2014, **9**, 166–178.

4 C.-L. Wang, C.-Q. Song, W.-H. Shen, Y.-Y. Qi, Y. Xue, Y. C. Shi, H. Yu and L. Feng, *Catal. Sci. Technol.*, 2019, **9**, 1769–1773.

5 N. V. Shevchuk, K. Liubchak, K. G. Nazarenko, A. A. Yurchenko, D. M. Volochnyuk, O. O. Grygorenko and A. A. Tolmachev, *Synthesis*, 2012, **44**, 2041–2048.

6 J. Conesa-Egea, J. Gallardo-Martínez, S. Delgado, J. I. Martínez, J. Gonzalez-Platas, V. Fernández-Moreira, U. R. Rodríguez-Mendoza, P. Ocón, F. Zamora and P. Amo-Ochoa, *Small*, 2017, **13**, 1700965.

7 P. Amo-Ochoa, K. Hassanein, C. J. Gómez-García, S. Benmansour, J. Perles, O. Castillo, J. I. Martínez, P. Ocón and F. Zamora, *Chem. Commun.*, 2015, **51**, 14306–14309.

8 K. Hassanein, J. Conesa-Egea, S. Delgado, O. Castillo, S. Benmansour, J. I. Martínez, G. Abellán, C. J. Gómez-García, F. Zamora and P. Amo-Ochoa, *Chem. Eur. J.*, 2015, **21**, 17282–17292.

9 J. López, M. Murillo, G. Lifante-Pedrola, E. Cantelar, J. Gonzalez-Platas, U. R. Rodríguez-Mendoza and P. Amo-Ochoa, *CrystEngComm.*, 2022, **24**, 341–349.

10 M. Murillo, J. Álvarez-Conde, R. Wannemacher, J. Cabanillas-González, J. González-Platas, U. R. Rodríguez-Mendoza, A. Liang, R. Turnbull, D. Errandonea, J. I. Martínez and P. Amo-Ochoa, *J. Mater. Chem. C*, 2022, **10**, 18004–18016.

11 J. Conesa-Egea, Carlos. D. Redondo, J. I. Martínez, C. J. Gómez-García, Ó. Castillo, F. Zamora and P. Amo-Ochoa, *Inorg. Chem.*, 2018, **57**, 7568–7577.

12 M. Murillo, R. Wannemacher, J. Cabanillas-González, U. R. Rodríguez-Mendoza, J. Gonzalez-Platas, A. Liang, R. Turnbull, D. Errandonea, G. Lifante-Pedrola, A. García-Hernán, J. I. Martínez and P. Amo-Ochoa, *Inorg. Chem.*, 2023, **62**, 10928–10939.

13 J. Conesa-Egea, Carlos. D. Redondo, J. I. Martínez, C. J. Gómez-García, Ó. Castillo, F. Zamora and P. Amo-Ochoa, *Inorg. Chem.*, 2018, **57**, 7568–7577.